[CANCER RESEARCH 63, 7785–7790, November 15, 2003]

Determination of Clonality of Metastasis by Cell-Specific Color-Coded Fluorescent-Protein Imaging

Norio Yamamoto,[1,2,3] Meng Yang,[1] Ping Jiang,[1] Mingxu Xu,[1] Hiroyuki Tsuchiya,[3] Katsuro Tomita,[3] A. R. Moossa,[2] and Robert M. Hoffman[1,2]

[1]AntiCancer, Inc., San Diego, California; [2]Department of Surgery, University of California, San Diego, California; and [3]Department of Orthopedic Surgery, School of Medicine, Kanazawa University, Ishikawa, Japan

ABSTRACT

It has been thought that metastases are clonal and originate from rare cells in primary tumors that are heterogeneous in genotype and phenotype. Recent studies using DNA array analysis challenge this hypothesis and suggest the genetic background of the host is the important determinant of metastatic potential implying that metastases are not necessarily clonal. Previous methods to determine clonality of metastasis used karyotype or molecular analysis that were complicated, thereby limiting the number of metastatic colonies analyzed and the conclusions that could be drawn. We describe here the use of green fluorescent protein-labeled or red fluorescent protein-labeled HT-1080 human fibrosarcoma cells to determine clonality by simple fluorescence visualization of metastatic colonies after mixed implantation of the red and green fluorescent cells. Resulting pure red or pure green colonies were scored as clonal, whereas mixed yellow colonies were scored as nonclonal. In a spontaneous metastasis model originating from footpad injection in severe combined immunodeficient mice, 95% of the resulting lung colonies were either pure green or pure red, indicating monoclonal origin, whereas 5% were of mixed color, indicating polyclonal origin. In an experimental lung metastasis model established by tail vein injection in severe combined immunodeficient mice, clonality of lung metastasis was dependent on cell number. With a minimum cell number injected, almost all (96%) colonies were pure red or green and therefore monoclonal. When a large number of cells were injected, almost all (87%) colonies were mixed color and therefore heteroclonal. We conclude that spontaneous metastasis may be clonal because they are rare events, thereby supporting the rare-cell clonal origin of metastasis hypothesis. The clonality of the experimental metastasis model depended on the number of input cells. The simple fluorescence method of determining clonality of metastases described here can allow large-scale clonal analysis in numerous types of metastatic models.

INTRODUCTION

Tumors have been thought to consist of subpopulations of cells with only rare cells capable of metastasizing (1–3). To produce a metastasis, a cancer cell must undergo a series of sequential steps, including detachment from the solid tumor, invasion, intravasation, survival in the circulation, extravasation, initiation of proliferation in the target organ, angiogenesis, and evasion of host defenses with eventual metastatic colony formation (1–4). Successful completion of all these steps depends on both tumor cell properties as well as host factors (2). Few tumor cells are thought to be able to complete all these steps, and therefore, metastasis was thought to be an inefficient and rare process (5). For example, the presence of tumor cells in the circulation does not predict the eventual formation of metastases (5).

Previous experimental protocols to determine clonality were complex, thereby limiting their resolution and extent of analysis. For example, radiolabeled murine B16 melanoma cells were used to determine metastatic frequency. After i.v. injection in mice, $<0.1\%$ of the original inoculum produced colonies on the lung (5).

Clones selected from the parent B16 tumor were found to differ extensively in their ability to form metastases. It was concluded that only rare cells with high metastatic potential are present within the parental cell population before their injection into animals (3).

Using induced chromosomal aberrations as markers, the same chromosomal abnormality was found in all cells examined of individual metastases in the B16 model. However, metastases differed from one another in that they had different chromosomal markers. These findings indicated that the metastases were clonal but that they probably originated from different progenitor cells (2). Even when heterogeneous clumps of tumor cells were injected, the individual metastases exhibited a karyotype unique to one metastatic cell type (6). Clonal analysis of metastases produced by a B16 melanoma line containing different drug resistance markers demonstrated that $>80\%$ of experimental metastases produced by i.v. injection of tumor cells are of unicellular origin (7).

Retrovirus vector infection was also used to introduce unique genetic markers to a tumor cell populations (8). Despite the heterogeneity of the primary tumor at early stages of growth with regard to retroviral integration sites, advanced primary tumors consisted of a small number (<10) of distinct clones (8). Analysis of the resulting lung metastases demonstrated that they were derived from one of the few dominant primary tumor clones. In some animals, all of the lung metastases were derived from a common progenitor clone, whereas in others, each metastatic nodule had a different progenitor. This model showed that metastases are of clonal origin, but in this case, selection or clonal dominance occurred in the primary tumor (8). This method was also used to indicate that clonal dominance occurred at the metastatic site (9).

Analysis of the metastatic targeting of circulating tumor emboli showed that multicellular aggregates (homotypic or heterotypic) are more likely to give rise to a metastasis than a single tumor cell (2). However, the resulting metastases are clonal, suggesting either that metastases result from the proliferation of a single viable cell within a heterogeneous embolus or that a circulating tumor embolus is likely to be homogeneous because it originated from a clonal zone of a primary neoplasm (2).

Metastasis, therefore, appears to result from the selective growth of specialized subpopulations of cells that preexist in the parent tumor (5).

Recently, a small set of 17 genes was reported to predict metastatic potential for a variety of solid tumors using microarray gene expression analysis (10), suggesting that most primary tumor cells in a metastatic tumor express a metastasis signature. Bernards and Weinberg (11) suggested that combinations of early oncogenic alterations, not specific events, promote and determine metastatic potential in the primary tumor. This hypothesis suggests that metastases are not necessarily clonal.

In support of the hypothesis that the metastatic potential of the primary tumor is intrinsically determined by the host, significant differences in metastatic efficiency (as much as 10-fold) were found between the hosts in a transgenic tumor model without altering tumor

Received 7/26/03; accepted 9/9/03.

Grant support: National Cancer Institute Grant 1 R43 CA89779 (to AntiCancer, Inc.).

The costs of publication of this article were defrayed in part by the payment of page charges. This article must therefore be hereby marked *advertisement* in accordance with 18 U.S.C. Section 1734 solely to indicate this fact.

Requests for reprints: Robert M. Hoffman, AntiCancer, Inc., San Diego, CA 92111. Phone: (858) 654-2555; Fax: (858) 268-4175; E-mail: all@anticancer.com.

Table 1 *Clonal analysis of metastasis*

Type of metastasis	Experimental system (tagging method)	Method to analyze matastasis	Clonal or nonclonal metastasis	Reference no.
Experimental	Melanoma (Mixture of drug resistant and sensitive cells)	Phenotyping for drug sensitivity	Clonal	7
	Melanoma (X-irradiation to make chromosomal markers)	Karyotyping	Clonal	6
Low cell number injected	Human fibrosarcoma (GFP & RFP labeling)	Color coding	Clonal	Present study
High cell number injected	Human fibrosarcoma (GFP & RFP labeling)	Color coding	Nonclonal	Present study
Spontaneous	Melanoma (X-irradiation to make chromosomal markers)	Karyotyping	Clonal	2
	Human mammary cancer (Retroviral insertion)	Southern blotting	Clonal dominance of metastasis	9
	Mouse mammary cancer (Retroviral insertion)	Southern blotting	Clonal dominance of primary tumor	8
	Human adenocarcinoma (Gene expression pattern)	Microarray	Clonal dominance of primary tumor?	10
	Human fibrosarcoma (GFP & RFP labeling)	Color coding	Clonal	Present study

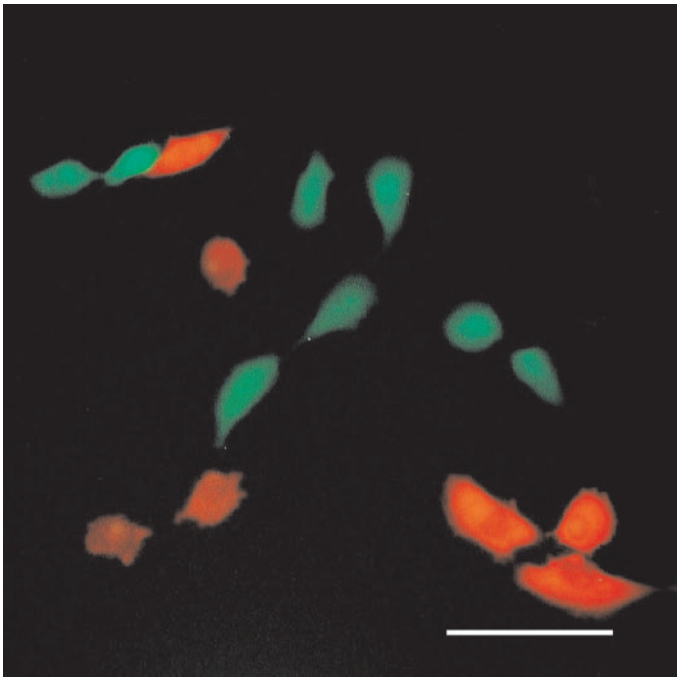

Fig. 1. Stable high GFP expressing human fibrosarcoma cells (HT-1080-GFP) and RFP expressing human fibrosarcoma cells (HT-1080-RFP) *in vitro*. Human fibrosarcoma cells (HT-1080) were transduced with GFP and the neomycin-resistance gene or RFP and the neomycin resistance gene in a retrovirus vector. Bright GFP-expressing cells (HT-1080-GFP) or RFP-expressing cells (HT-1080-RFP) were selected with G418 up to 800 μg/ml. Please read "Materials and Methods" for details. *A*, HT-1080-GFP; *B*, HT-1080-RFP. *Bars*, 100 μm.

initiation or growth kinetics (12, 13). These experiments suggest that the host genetic background plays a large role in determining metastasis and that metastases are not necessarily clonal.

In summary, two competing hypotheses of metastases have been put forward with one suggesting rare subpopulations of primary tumor cells have accumulated the numerous alterations required for metastasis, which would be mostly clonal (14), and the other suggesting most cells in a metastatic tumor are capable of metastasis, indicating that metastasis is not necessary clonal (15). Please see Table 1 for a summary of methods used to determine the clonal status of metastasis.

To develop a very simple, rapid, and high-resolution method to determine clonality of metastasis, we have used the GFP[4] or RFP to tag clones of the human fibrosarcoma cell line, HT-1080. Upon mixed implantation of red and green fluorescent cells, fluorescent metastatic colonies result that are either pure red or pure green, indicating clonality or yellow indicating mixed origin. GFP and RFP fluorescence enable dual-color imaging upon simultaneous excitation (16). Fluorescent protein imaging enables the visualization of metastasis both *ex vivo* and by whole-body imaging (17–26). With this new method, we report the clonal status of lung metastases of the HT-1080 line in SCID mice that were formed spontaneously or experimentally.

MATERIALS AND METHODS

Production of GFP and RFP Retrovirus (25). The pLEIN retroviral vector (Clontech Laboratories, Inc., Palo Alto, CA) expressing GFP and the neomycin resistance gene on the same bicistronic message was used as a GFP expression vector. PT67, an NIH3T3-derived packaging cell line, expressing the 10 Al viral envelope, was purchased from Clontech Laboratories, Inc. PT67 cells were cultured in DMEM (Irvine Scientific, Santa Ana, CA) supplemented with 10% heat-inactivated fetal bovine serum (Gemini Bio-products, Calabasas, CA). For vector production, packaging cells (PT67), at 70% confluence, were incubated with a precipitated mixture of DOTAP reagent (Boehringer Mannheim, Indianapolis, IN) and saturating amounts of pLEIN plasmid for 18 h. Fresh medium was replenished at this time. The cells were examined by fluorescence microscopy 48 h after transduction. For selection, the cells were cultured in the presence of 500-2000 μg/ml G418 (Life Technologies, Inc., Grand Island, NY) for 7 days to select for a clone producing high amounts of a GFP retroviral vector (PT67-GFP).

For RFP retrovirus production, The *Hin*dIII/*Not*I fragment from pDsRed2 (Clontech), containing the full-length RFP cDNA, was inserted into the *Hin*dIII/*Not*I site of pLNCX2 (Clontech) that has the neomycin resistance gene to establish the pLNCX2-DsRed2 plasmid. The PT67 cells, at 70% confluence, were incubated with a precipitated mixture of Lipofectamine reagent (Life Technologies, Inc.) and saturating amounts of pLNCX2-DsRed2 plasmid as described above for GFP vector production. For selection of a clone producing high amounts of a RFP retroviral vector (PT67-DsRed2), the cells were cultured in the presence of 200-1000 μg/ml G418 for 7 days (25, 26).

GFP and RFP Gene Transduction of HT-1080 Fibrosarcoma Cells. For GFP or RFP gene transduction, 70% confluent human HT-1080 human fibrosarcoma cells (American Type Culture Collection, Manassas, VA), were

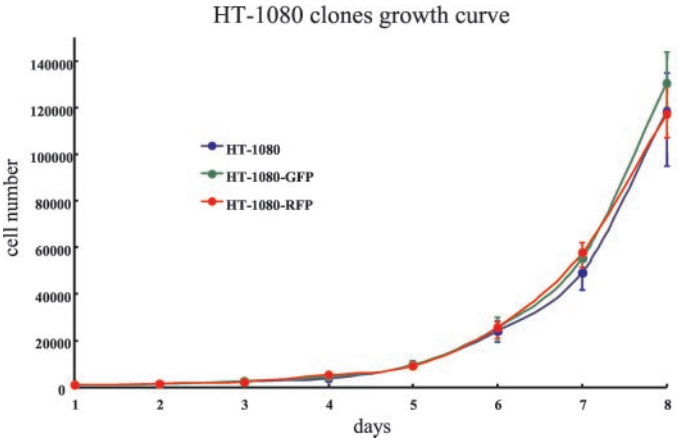

Fig. 2. Cell proliferation potential of parental and fluorescent-protein expressing clones. Three culture dishes for each clone (parental HT-1080, HT-1080-GFP, HT-1080-RFP) were used to count the cell number for 8 days. *Filled circle* shows average cell number for each group. *Bars* show the range of measurement at each time point.

[4] The abbreviations used are: GFP, green fluorescent protein; RFP, red fluorescent protein; SCID, severe combined immunodeficient.

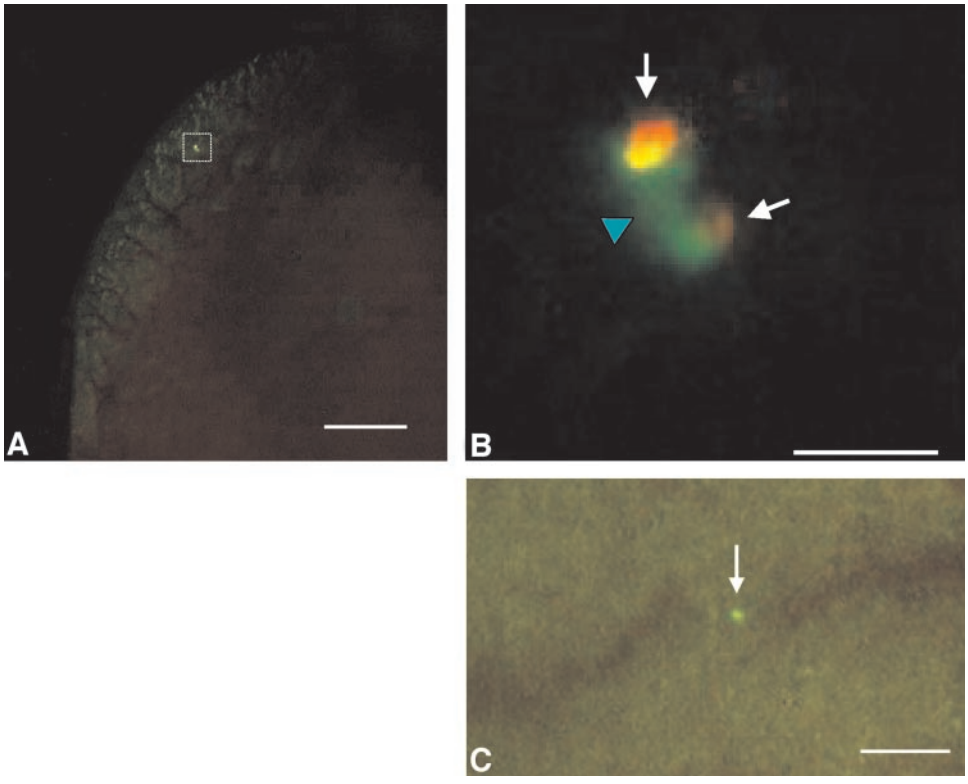

Fig. 3. Clonal status of spontaneous lung micrometastasis 6 weeks after cell implantation in the footpad. *A*, low magnification view of excised lung 6 weeks after footpad injection. The *white squares* indicate the area in which the high magnification view is shown as *B*. *Bar*, 1 mm. *B*, high magnification view of spontaneous lung micrometastasis indicated in *A*. *White arrows* indicate red fluorescent cells and *blue arrowhead* indicates green fluorescent cells. *Bar*, 100 μm. *C*, single cell spontaneous lung metastasis observed in footpad injection model. Green fluorescent single cells are observed in lung microcapillaries. *White arrow* indicates single cell. *Bar*, 200 μm.

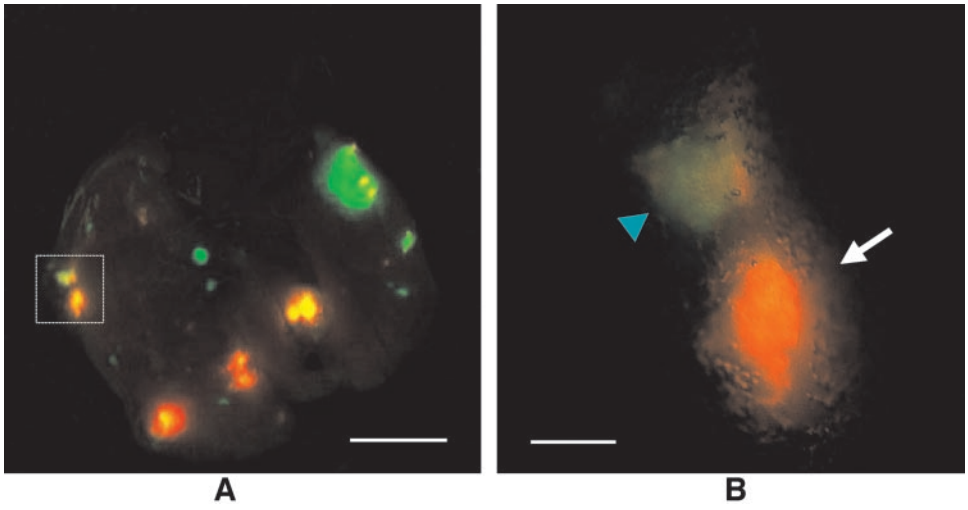

Fig. 4. Clonal status of spontaneous lung metastases 8 weeks after cell implantation. *A*, low magnification view of the excised lung 8 weeks after footpad injection. *White square* indicates the area in which the high magnification view is shown as *B*. *Bar*, 5 mm. *B*, high magnification view of spontaneous lung metastases indicated in *A*. *White arrow* indicates a spontaneous lung metastatic colony showing pure red fluorescent color. *Blue arrowhead* indicates a rare spontaneous lung metastatic colony showing mixed green and red fluorescent colors. *Bar*, 800 μm.

incubated with a 1:1 precipitated mixture of retroviral supernatants of PT67-GFP or PT67-DsRed2 cells and RPMI 1640 (Mediatech, Inc., Herndon, VA) containing 10% fetal bovine serum for 72 h. Fresh medium was replenished at this time. Cells were harvested by trypsin/EDTA 72 h after transduction and subcultured at a ratio of 1:15 into selective medium, which contained 200 μg/ml G418. The level of G418 was increased stepwise up to 800 μg/ml. Clones of HT-1080 expressing high levels of GFP (HT-1080-GFP) or RFP (HT-1080-RFP) were isolated with cloning cylinders (Bel-Art Products, Pequannock, NJ) using trypsin/EDTA and amplified by conventional culture methods.

Cell Proliferation Rate Determination. Each fluorescent-tagged HT-1080 clone (HT-1080-GFP or HT-1080-RFP) and parental clone (HT-1080) was seeded at a density of 1×10^3 cells/dish in 100-mm dishes in RPMI 1640 (day 1). The dishes were kept in an incubator at 37°C and 5% CO_2. Every other day, from days 2 to 8, three dishes for each clone were used to count cells. Resuspended cells collected by conventional methods were stained with trypan blue (Sigma) for viability. Viable cells were counted with a hemocytometer (Reichert Scientific Instruments, Buffalo, NY).

Spontaneous Metastasis Footpad Injection Model. Six-week-old, female, SCID mice were used for all *in vivo* studies. HT-1080-GFP cells and HT-1080-RFP cells were first harvested by trypsinization and 3×10^6 cells of

Table 2 *Clonal analysis of metastasis by fluorescence-tagged color coding*

	Total number (±SD for individual)		
	Green	Red	Mixed
Spontaneous metastasis model (footpad injection) $n = 12$	250 (± 13.0)	263 (± 9.5)	29 (± 1.5)
	Percentage of mixed color colonies (nonclonal): 5.4%		
Experimental metastasis model (min. cell no. tail vein injection) $n = 11$	205 (± 10.7)	241 (± 12.0)	17 (± 1.8)
	Percentage of mixed color colonies (nonclonal): 3.7%		
Experimental metastasis model (large cell no. tail vein injection) $n = 10$	116 (± 4.5)	100 (± 5.7)	1628 (± 28.3)
	Percentage of mixed color colonies (nonclonal): 86.7%		

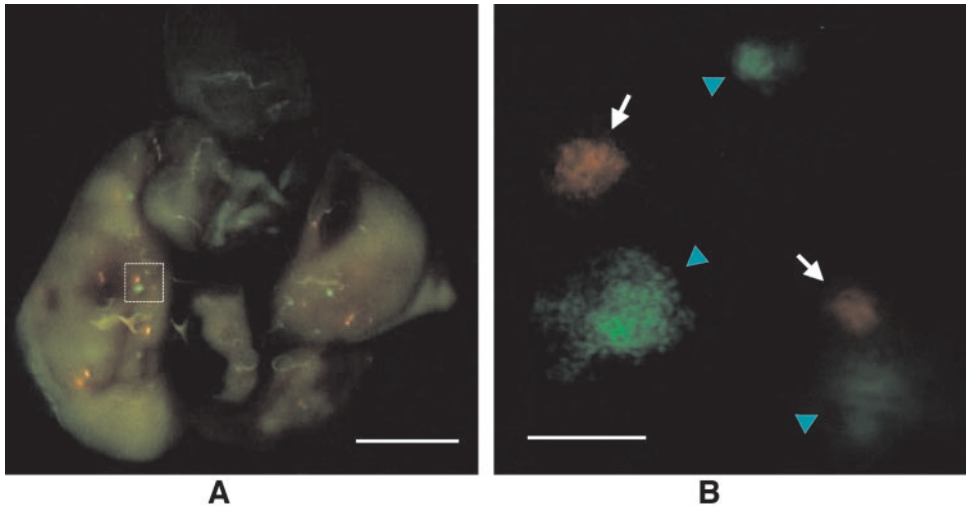

Fig. 5. Clonal status of experimental lung metastases with minimum input cell number. *A*, low magnification view of the excised lung. *White square* indicates high magnification area. *Bar*, 5 mm. *B*, high magnification view of the metastases. *White arrows* indicate pure red fluorescent colonies. *Blue arrowhead* indicates pure green fluorescent colonies. *Bar*, 250 μm.

each clone were mixed well with each other. The cells were washed three times with serum-free cold medium. Twenty SCID mice were injected with 6×10^6 cells (3×10^6 cells from each clone) in a total volume of 50 μl into the right hind footpad. Cells were injected within 30 min of harvest. Five mice were sacrificed for visualization of the early stage of lung metastasis. The rest of the experimental animals were sacrificed 8 weeks after injection and spontaneous lung metastases on the excised lungs were observed under fluorescence microscopy. The colonies that were $>$200 μm in diameter were counted and evaluated for clonality, with pure red and green colonies determined to be clonal and mixed yellow color, nonclonal.

Tail Vein Injection Experimental Metastasis Model. To determine the minimum cell number to establish lung metastasis by tail vein injection, a total 1×10^4, 5×10^4, 1×10^5, 5×10^5 and 1×10^6 cells, consisting of an equal number of HT-1080-GFP cells and HT-1080-RFP cells, were resuspended in 200 μl of PBS and injected into the tail vein. Three SCID mice were used for each cell concentration. Two weeks after cell injection,

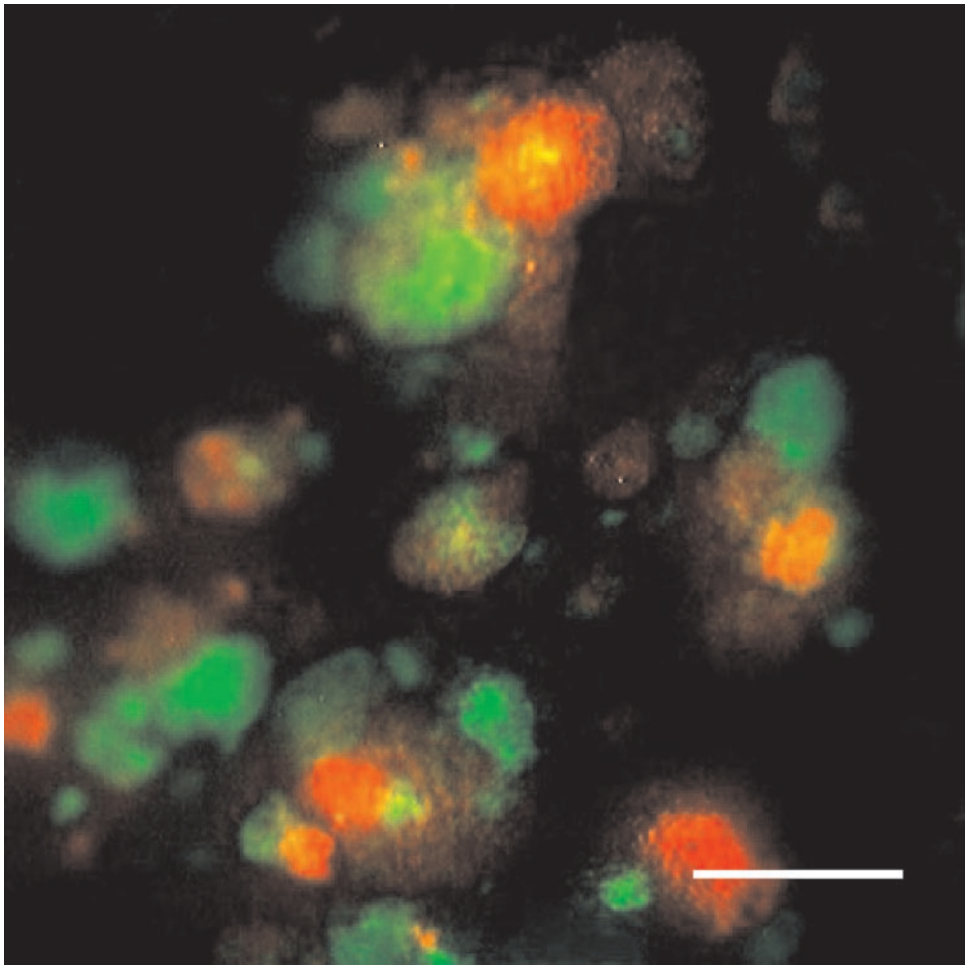

Fig. 6. Clonal status of experimental lung metastases with large input cell number. High magnification view of the excised lung. Most of the colonies show mixed color. *Bar*, 1 mm.

the mice were sacrificed, and lung metastases were evaluated under fluorescence microscopy.

Subsequently, 1×10^5 cells were found to be the minimum cell number to produce metastases. A total of 1×10^5 cells of each clone was then resuspended in 200 μl of PBS and injected into the tail vein to evaluate clonality in the experimental lung metastasis model with a minimum input cell number conditions. Fifteen SCID mice were used for this experiment. Fifteen days after cell injection, the mice were sacrificed, and the lungs were removed. The status and number of lung colonies were visualized under fluorescence microscopy. The colonies that were >200 μm in diameter were counted and evaluated for clonality by color purity as described above.

The clonality of experimental lung metastasis with a large input cell number was also evaluated. Twenty SCID mice were injected with 2×10^6 cells (1×10^6 RFP and 1×10^6 GFP cells) in a total volume of 200 μl into the tail vein. Cells were injected within 30 min of harvest. Immediately after the injection (day 1), 3 mice were sacrificed, and the tumor cell emboli in the microcapillaries on the lung surface were visualized under fluorescence microscopy. On days 6 and 11 after cell injection, 3 mice were sacrificed, and the metastatic colonies on the excised lungs were visualized under fluorescence microscopy for pure or mixed color. On day 16, 11 mice were sacrificed, and the lungs were removed to evaluate the lung colonies for pure or mixed color.

Fluorescence Optical Imaging. Images were captured directly with a Hamamatsu C5810 3CCD camera (Hamamatsu Photonics, Bridgewater, NJ). For macroimaging, a fluorescence light box (Lightools Research, Encinitas, CA) was used. For microimaging, a Leica fluorescence stereo microscope model LZ12 was coupled with the charge-coupled device (CCD) camera. This microscope was equipped with a GFP filter set and a mercury lamp with a 50-W power supply. Images were processed for contrast and brightness and analyzed with the use of Image ProPlus 3.1 software. High-resolution images of 1024×724 pixels were captured directly on an IBM PC (25, 26).

All animal studies were conducted in accordance with the principles and procedures outlined in the "NIH Guide for the Care and Use of Laboratory Animals" under assurance number A3873-1. Animals were kept in a barrier facility under HEPA filtration. Mice were fed with autoclaved laboratory rodent diet (Teckland LM-485; Western Research Products, Orange, CA).

RESULTS AND DISCUSSION

Cell Proliferation of Unlabeled GFP- and RFP-Expressing Clones. The selected fluorescent-protein transduced HT-1080 cells have a strikingly bright GFP or RFP fluorescence *in vitro* (Fig. 1). All cells in the population expressed GFP or RFP, indicating stability of the transgene. There was no difference in the proliferation rate of parental unlabeled HT-1080 and selected HT-1080-GFP or HT-1080-RFP cells as determined in monolayer culture (Fig. 2).

Clonality of Spontaneous Metastasis. At 6 weeks after injection, micrometastasis comprising single or several cells could be visualized under fluorescence microscopy (Fig. 3, *A–C*). Micrometastatic clusters of RFP cells attached to each other by intervening GFP cells were also visualized (Fig. 3*B*), demonstrating that mixed emboli could invade from the primary site and reach the lung as a cluster. Twelve of 15 SCID mice had primary footpad tumors and spontaneous metastases on the lungs 8 weeks after footpad injection. However, almost all of the lung metastatic colonies in this spontaneous metastasis

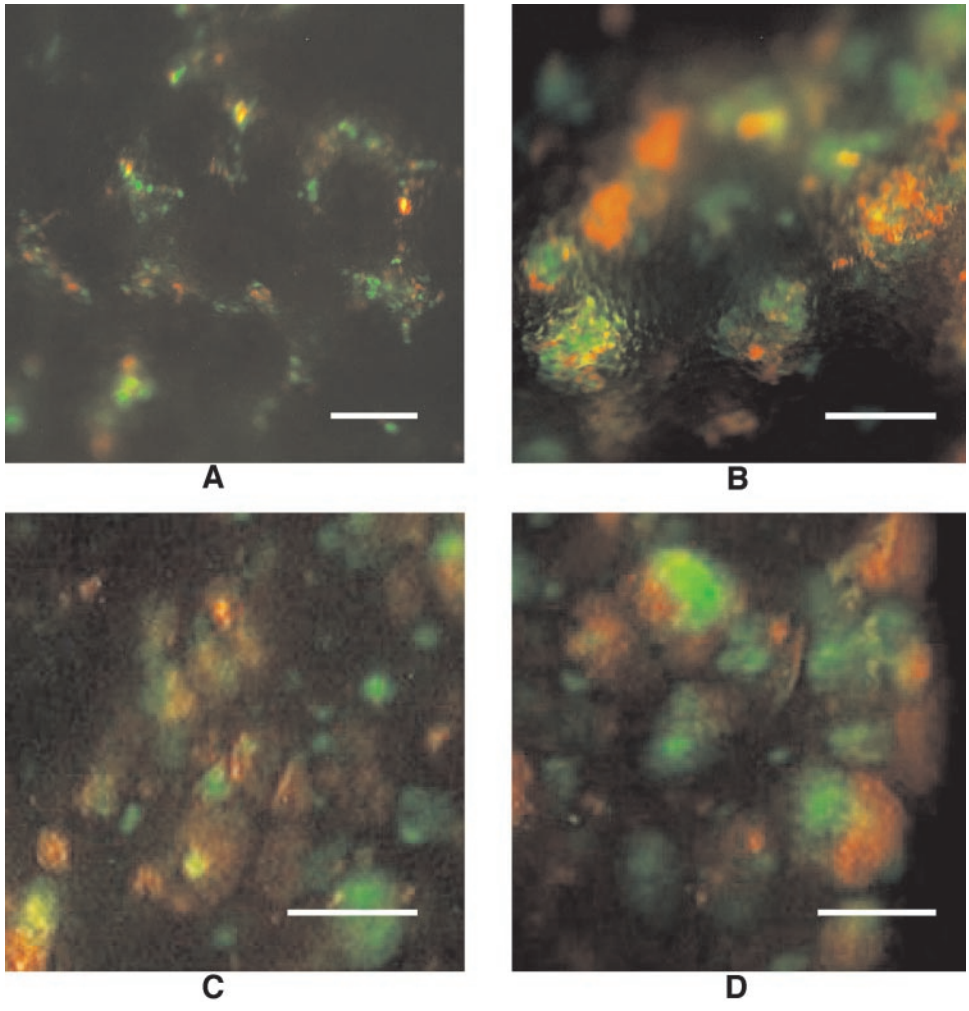

Fig. 7. Development of colonies of experimental lung metastasis with large input cell number. Metastases on the excised lung were imaged under fluorescence microscopy at each time point: *A*, immediately after tail vein injection (day 1). *Bar*, 200 μm. *B*, day 6. *Bar*, 250 μm. *C*, day 11. *Bar*, 300 μm. *D*, day 16. *Bar*, 400 μm.

model were pure green or red as visualized (Fig. 4*A*). Green and red colonies were found approximately at the same ratio on the lung surface (Table 2). Only 5% of the colonies were of mixed color (Table 2, Fig. 4*B*). Although mixtures of GFP- and RFP-labeled clones were injected in the same footpad, the resulting lung metastatic colonies seem to be ultimately derived from single cells, even if seeded as mixed emboli. The data suggest most of the metastatic colonies were clonal.

Clonality of Experimental Metastasis with Low Input Cell Number. The SCID mice that were injected i.v. with $<1 \times 10^5$ cells had no resulting lung metastasis (data not shown). When 2×10^5 cells were injected, 11 of 15 mice had lung metastases. Almost all lung colonies were pure green or red, similar to the spontaneous metastasis model (Table 2, Figs. 5, *A* and *B*). However, in contrast to the metastatic colonies in the spontaneous metastasis model that varied greatly in size, the experimental metastatic colonies were of similar size. Although a minimum number of cells injected was necessary to form metastasis, this minimum number led to clonal metastases as observed by their pure color. If a significant number of colonies were derived from several cells, more colonies would have been of mixed yellow color than what was observed.

Clonality of Experimental Metastasis with Large Input Cell Number. One day after tail vein injection of 2×10^6 GFP and RFP HT-1080 cells (Fig. 6), mixed emboli in lung microcapillaries were visualized when the animals were sacrificed immediately after injection (Fig. 7*A*). When animals were sacrificed at days 6, 14, and 16, most colonies on the extracted lung were nonclonal mixtures (Fig. 7*B*, *C*, and *D*). In some colonies, one color was underrepresented, suggesting that not every cell participated in colony formation and that some cells grew better than others in the initial seeding embolism. Almost all colonies showed mixed color in this model (Figs. 6 and 7 and Table 2) and were therefore determined to be nonclonal.

In summary, the lung colonies were mostly clonal in the spontaneous metastasis model, even if initial emboli were not clonal. However, in the experimental metastasis model, the clonality of colonies established on the lung were strongly affected by the number of injected cells. To obtain clonal experimental metastasis such as from a high-metastasis clone, the number of injected cells should be limited.

With the methods described in this article, clonality of metastasis can be evaluated under any condition and model system. For example, cells with specific genotypes such as those containing metastasis signatures (10, 11) mentioned above can be specifically labeled with one color fluorescent protein and cells without the metastasis signature labeled with another color fluorescent protein. Mixed injection will determine the relative metastatic properties of cells with such genetic signatures. The fluorescence color-coding method described here should enable the determination of relative metastatic capability of any cancer cells with gene(s) of interest.

REFERENCES

1. Cotran, R. S., Kumar, V., and Robbins, S. L. Pathological Basis of Cancer, Ed. 5. Philadelphia: W. B. Saunders Company, 1994.
2. Talmadge, J. E., Wolman, S. R., and Fidler, I. J. Evidence for the clonal origin of spontaneous metastasis. Science (Wash. DC), *217:* 361–363, 1982.
3. Fidler, I. J., and Kripke, M. L. Metastasis results from preexisting variant cells within a malignant tumor. Science (Wash. DC), *197:* 893–895, 1977.
4. Kuo, T-H., Kubota, T., Watanabe, M., Furukawa, T., Teramoto, T., Ishibiki, K., Kitajimi, M., Moossa, A. R., Penman, S., and Hoffman, R. M. Liver colonization competence governs colon cancer metastasis. Proc. Natl. Acad. Sci. USA, *92:* 12085–12089, 1995.
5. Fidler, I. J., and Hart, I. R. Biological diversity in metastatic neoplasms. Origins and implications. Science (Wash. DC), *217:* 998–1003, 1982.
6. Fidler, I. J., and Talmadge, J. E. Evidence that intravenously derived murine pulmonary metastases can originate from the expansion of a single tumor cell. Cancer Res., *46:* 5167–5171, 1986.
7. Poste, G., Tzeng, J., Doll, J., Greig, R., Rieman, D., and Zeidman, I. Evolution of tumor cell heterogeneity during progressive growth of individual lung metastases. Pro. Natl. Acad. Sci. USA, *79:* 6574–6578, 1982.
8. Korczak, B., Robson, I. B., Lamarche, C., Bernstein, A., and Kerbel, R. S. Genetic tagging of tumor cells with retrovirus vectors: clonal analysis of tumor growth and metastasis *in vivo*. Mol. Cell. Biol., *8:* 3143–3149, 1988.
9. Cornetta, K., Moore, A., Johannessohn, M., and Sledge, G. W. Clonal dominance detected in metastases but not primary tumors of retrovirally marked human breast carcinoma injected into nude mice. Clin. Exp. Metastasis, *12:* 3–12, 1994.
10. Ramaswamy, S., Ross, K. N., Lander, E. S., and Golub, T. R. A molecular signature of metastasis in primary solid tumors. Nat. Genet., *33:* 49–54, 2003.
11. Bernards, R., and Weinberg, R. A. A progression puzzle. Nature (Lond.), *418:* 823, 2002.
12. Lifsted, T., Le Voyer, T., Williams, M., Muller, W., Klein-Szanto, A., Buetow, K. H., and Hunter, K. W. Identification of inbred mouse strains harboring genetic modifiers of mammary tumor age of onset and metastatic progression. Int. J. Cancer, *77:* 640–644, 1998.
13. Hunter, K. W., Broman, K. W., Voyer, T. L., Lukes, L., Cozma, D., Debies, M. T., Rouse, J., and Welch, D. R. Predisposition to efficient mammary tumor metastatic progression is linked to the breast cancer metastasis suppressor gene Brms1. Cancer Res., *61:* 8866–8872, 2001.
14. Fidler, I. J., and Kripke, M. L. Genomic analysis of primary tumors does not address the prevalence of metastatic cells in the population. Nat. Genet., *34:* 23, 2003.
15. Hunter, K., Welch, D. R., and Liu, E. T. Genetic background is an important determinant of metastatic potential. Nat. Genet., *34:* 23–24, 2003.
16. Jakobs, S., Subramaniam, V., Schonle, A., Jovin, T. M., and Hell, S. W. EFGP and DsRed expressing cultures of *Escherichia coli* imaged by confocal, two-photon and fluorescence lifetime microscopy. FEBS Lett., *479:* 131–135, 2000.
17. Chishima, T., Miyagi, Y., Wang, X., Yamaoka, H., Shimada, H., Moossa, A. R., and Hoffman, R. M. Cancer invasion and micrometastasis visualized in live tissue by green fluorescent protein expression. Cancer Res., *57:* 2042–2047, 1997.
18. Chishima, T., Miyagi, Y., Wang, X., Tan, Y., Shimada, H., Moossa, A. R., and Hoffman, R. M. Visualization of the metastatic process by green fluorescent protein expression. Anticancer Res., *17:* 2377–2384, 1997.
19. Chishima, T., Miyagi, Y., Wang, X., Baranov, E., Tan, Y., Shimada, H., Moossa, A. R., and Hoffman, R. M. Metastatic patterns of lung cancer visualized live and in process by green fluorescence protein expression. Clin. Exp. Metastasis, *15:* 547–552, 1997.
20. Chishima, T., Yang, M., Miyagi, Y., Li, L., Tan, Y., Baranov, E., Shimada, H., Moossa, A. R., Penman,, S., and Hoffman, R. M. Governing step of metastasis visualized *in vitro*. Proc. Natl. Acad. Sci. USA *94:* 11573–11576, 1997.
21. Yang, M., Hasegawa, S., Jiang, P., Wang, X., Tan, Y., Chishima, T., Shimada, H., Moossa, A. R., and Hoffman, R. M. Widespread skeletal metastatic potential of human lung cancer revealed by green fluorescent protein expression. Cancer Res., *58:* 4217–4221, 1998.
22. Yang, M., Jiang, P., Sun, F. X., Hasegawa, S., Baranov, E., Chishima, T., Shimada, H., Moossa, A. R., and Hoffman, R. M. A fluorescent orthotopic bone metastasis model of human prostate cancer. Cancer Res., *59:* 781–786, 1999.
23. Yang, M., Chishima, T., Wang, X., Baranov, E., Shimada, H., Moossa, A. R., and Hoffman, R. M. Multi-organ metastatic capability of Chinese hamster ovary cells revealed by green fluorescent protein (GFP) expression. Clin. Exp. Metastasis, *17:* 417–422, 1999.
24. Yang, M., Baranov, E., Jiang, P., Sun, F. X., Li, X. M., Li, L., Hasegawa, S., Bouvet, M., Al-Tuwaijri, M., Chishima, T., Shimada, H., Moossa, A. R., Penman, S., and Hoffman, R. M. Whole-body optical imaging of green fluorescent protein-expressing tumors and metastases. Proc. Natl. Acad. Sci. USA, *97:* 1206–1211, 2000.
25. Yang, M., Baranov, E., Wang, J. W., Jiang, P., Wang, X., Sun, F. X., Bouvet, M., Moossa, A. R., Penman, S., and Hoffman, R. M. Direct external imaging of nascent cancer, tumor progression, angiogenesis, and metastasis on internal organs in the fluorescent orthotopic model. Proc. Natl. Acad. Sci. USA, *99:* 3824–3829, 2002.
26. Yamamoto, N., Yang, M., Jiang, P., Tsuchiya, H., Tomita, K., Moossa, A. R., and Hoffman, R. M. Real-time GFP imaging of spontaneous HT-1080 fibrosarcoma lung metastases. Clin. Exp. Metastasis, *20:* 181–185, 2003.